Pho Engineering Success

Overview

Design

PhoB Regulon Signaling Pathway

Lambert iGEM's phosphate-sensitive biosensor is based on the Pho Regulon signaling pathway, native to *E. coli* cells (Figure 1.1). The pathway controls the expression of the Pho Regulon by responding to extracellular inorganic phosphate levels [1].

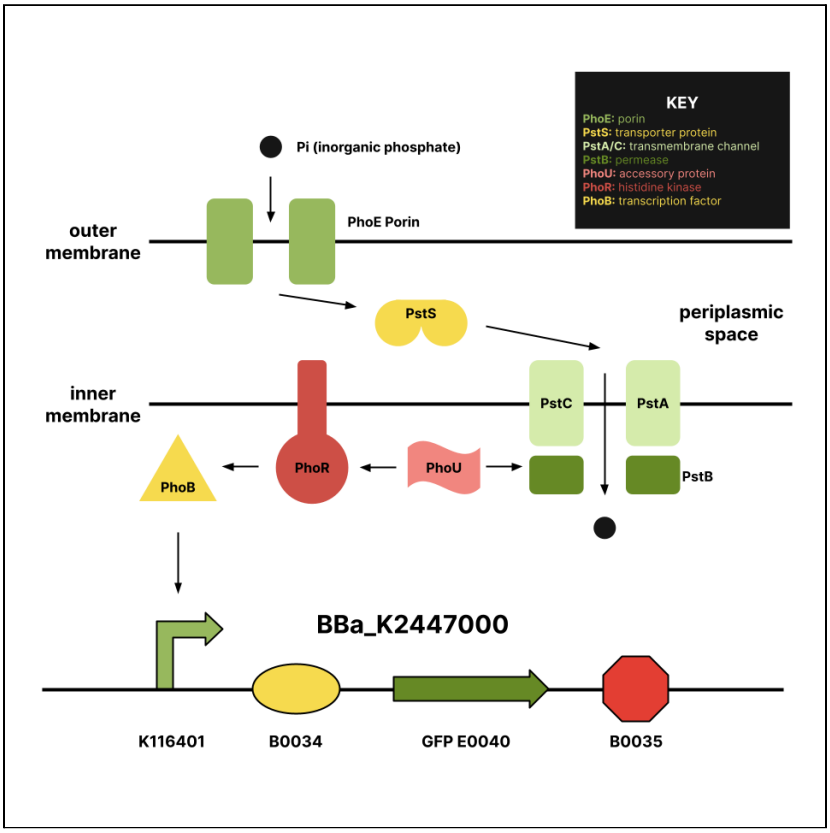

Figure 1.1 *Diagram of the Pho Regulon signaling pathway.*

First, inorganic phosphate (P_i) enters the cell by passing through PhoE porin channels in the outer membrane. Second, P_i binds to PstS, a transport protein, that carries P_i to the PstABC complex. The bound complex consists of the transmembrane channel PstA/C and the permease PstB, which phosphorylates PstA/C. Third, activated PstA/C transports P_i through the inner membrane.

After reading available literature, we found that high levels of P_i in the cytoplasm deactivate transcription of the Pho Regulon genes, creating an inverse relationship between extracellular P_i and the expression of downstream genes [2]. If there is a high presence of P_i, the molecule binds to PhoU, creating the PhoU-P_i complex. The complex then inhibits the permease PstB and histidine kinase PhoR. Next, PstB is no longer able to phosphorylate PstA/C, thus preventing P_i from entering the cell. As a result, PhoR is no longer able to phosphorylate the transcription factor PhoB, preventing the activation of the Pho Regulon promoter and expression of the Pho Regulon genes.

However, in lower levels of P_i, the molecule is less likely to interact with PhoU, enabling additional P_i to travel through PstA/C. Due to the absence of the PhoU-P_i complex, PhoR phosphorylates PhoB, later activating the Pho Regulon promoter and in turn allowing expression of the Pho Regulon genes.

BBa_K2447000 Design

Our 2020 team utilized NUS Singapore 2017 iGEM's part BBa_K2447000 in order to detect levels of extracellular P_i. While the inducible PhoB-activated promoter initiates expression of the downstream Pho Regulon genes, we replaced the natural genes with a GFP reporter, thereby allowing the construct to serve as an effective phosphate sensor. Low levels of extracellular phosphate allow PhoB to activate the promoter and subsequently trigger downstream expression of GFP. Inversely, high levels of extracellular phosphate prevent activation of PhoB and, therefore, inhibit the promoter.

The BBa_K2447000 construct is made up of four basic parts (Figure 1.2): a PhoB activated promoter (BBa_K116401), strong RBS (BBa_B0034), GFP reporter (BBa_E0040), and double terminator (BBa_B0015).

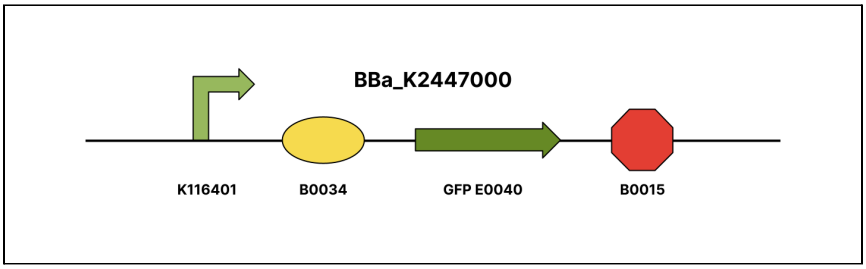

Figure 1.2 *Diagram of the BBa_K2447000 construct.*

Build

BBa_K2447000 Cloning Process

After ordering our insert on Integrated DNA Technologies (IDT), we hydrated and transformed our part into competent DH5-alpha *E. coli* cells. After attaining a purified stock of our part, we performed a restriction digest followed by a ligation with the pSB1C3 backbone. After transforming the complete plasmid into *E. coli* cells again, we purified and sequenced the part to confirm successful cloning (Figure 2.1).

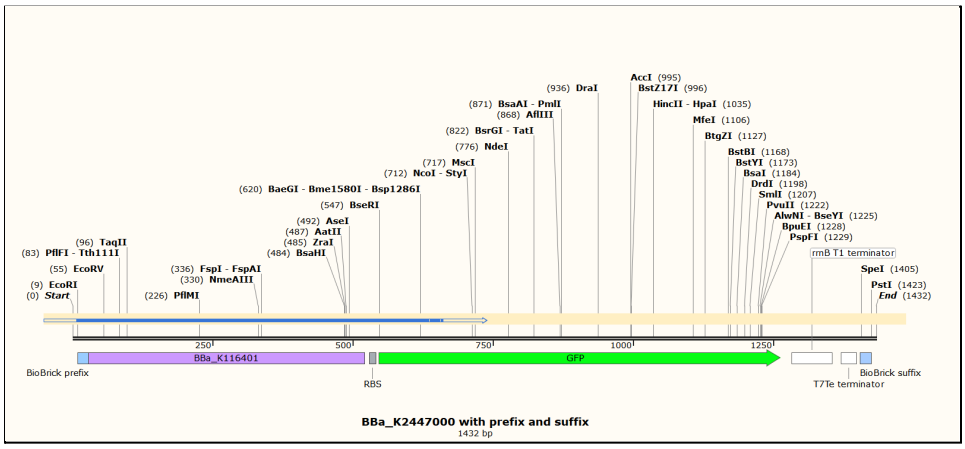

Figure 2.1 *Sequencing results confirming the successful cloning of the BBa_K2447000 part.*

Test

Modeling

Before beginning experimental testing of the phosphate biosensor, our team developed a deterministic Ordinary Differential Equation (ODE) model of the Pho Regulon utilizing MATLAB Simbiology (Figure 3.1). The model utilizes parameters within the Pho Regulon signaling pathway to predict the relationship between GFP expression and initial extracellular phosphate concentration for the phosphate sensor (Figure 3.2). Through the process of researching the Pho Regulon, finding different parameters such as rate constants, and inputting values, the team was able to create a model that represents the expected GFP values of the biosensor. The model served as a guide for characterization as the predicted GFP expression values were used to confirm the experimental results.

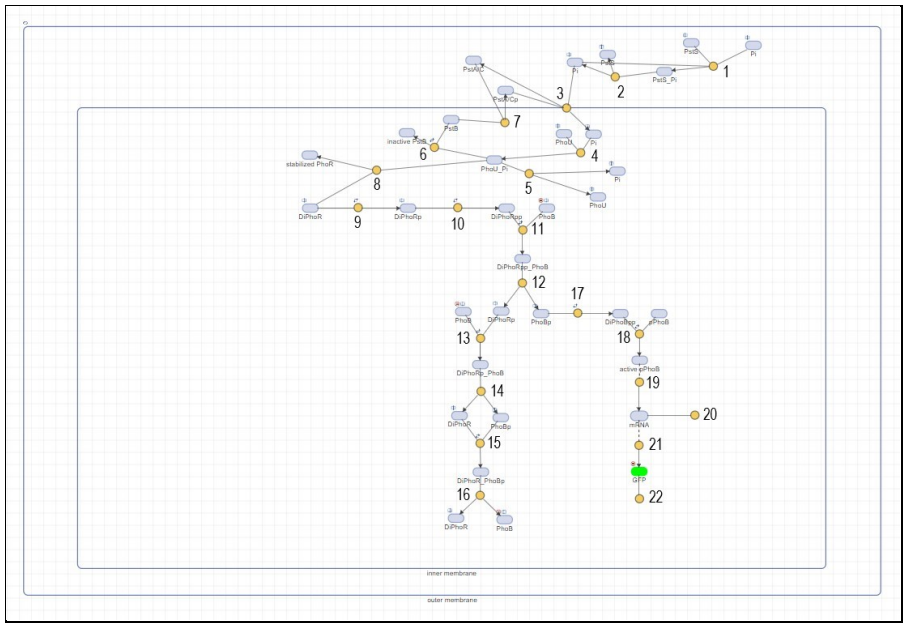

Figure 3.1 *Diagram of the reactions of the Pho Regulon signaling pathway in a single E. coli cell, created in MATLAB Simbiology software by our 2020 team.*

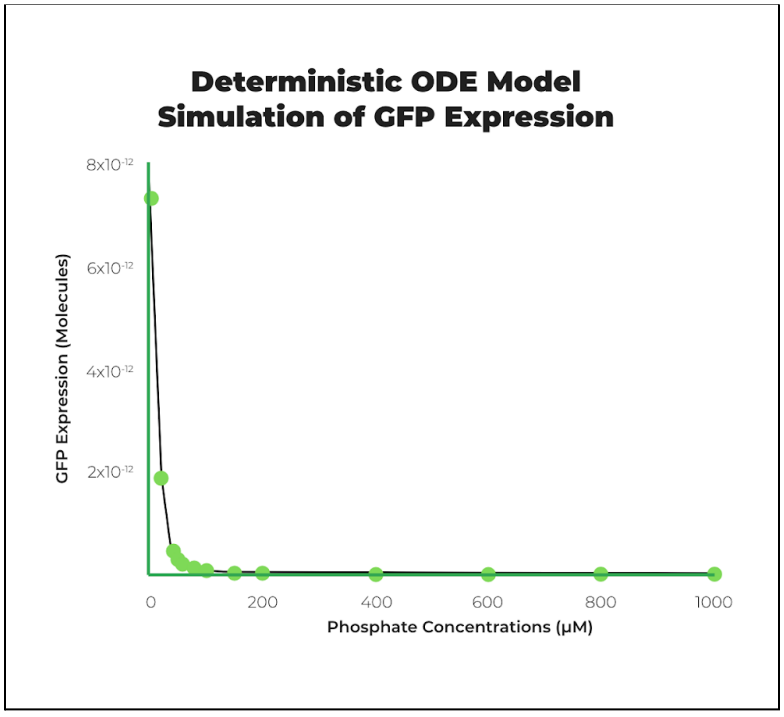

Figure 3.2 *Prediction of relationship between GFP expression and phosphate concentrations ranging from 0 to 100μM made by the deterministic ODE model by our 2020 team.*

Experimental Design

Upon completion of the model, our team created a plan for characterization. The biosensor cells were initially grown in 5mL of chloramphenicol LB for 24 hours. Then, they were re-inoculated into Erlenmeyer flasks containing 60mL of chloramphenicol LB in order to ensure that all flasks have a uniform concentration of cells. After overnight incubation, cell growth was measured using a spectrophotometer.

We found that the active growing range of *E. coli* cells is between OD_{600} values of 0.4 and 0.8. If OD_{600} was under 0.4, the cells were grown for longer until it reached active growth. On the other hand, if OD_{600} was greater than 0.8, the cells were diluted to desired OD_{600} with additional LB.

Then, the cells were resuspended into flasks. Taking 15mL from each flask, we transferred 5mL of the solution into three separate liquid culture tubes. The culture tubes were centrifuged down, and the LB supernatant was discarded. The resulting cell pellets were resuspended in 5mL of MOPS media, as MOPS contained significantly less phosphate than LB and ensured that phosphate in the LB would not affect the characterization data.

Next, 500μL of a specific phosphate concentration between 0μM to 100μM were added to each set of biological triplicates. The biosensor cells were grown for an additional 2 hours, and the OD_{600} and fluorescence values of the cells were quantified in a plate reader.

Characterization Results

We ran multiple trials of characterization with the protocol above and created a characterization curve utilizing the data obtained from the plate reader (Figure 3.3). While the data followed a negative trend from 0μM to 80μM, GFP expression began to increase unexpectedly as phosphate concentrations approached 100μM. As a whole, the characterization curve followed a non-linear path, making it difficult to properly assess the initial phosphate concentration of a sample.

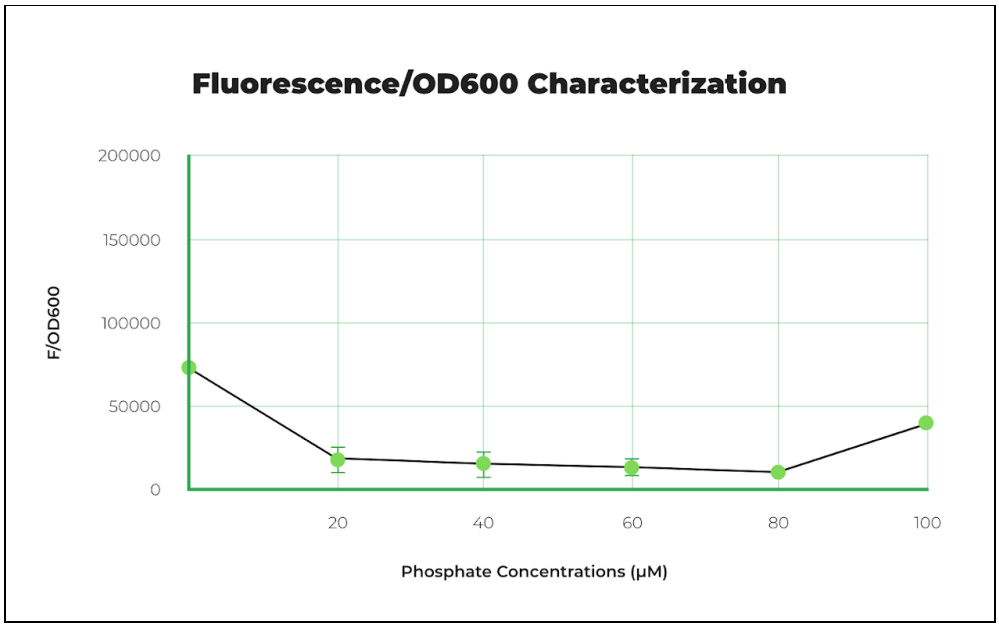

Figure 3.3 *BBa_K2447000 characterization curve showing the relationship between phosphate concentrations between 0µM to 100µM and fluorescence/OD$_{600}$.*

This abnormality at 100µM was further explored by increasing the range of phosphate concentrations to 150µM. However, the characterization curve yielded similar results: a non-linear negative trend with an irregular bump around 120µM (Figure 3.4).

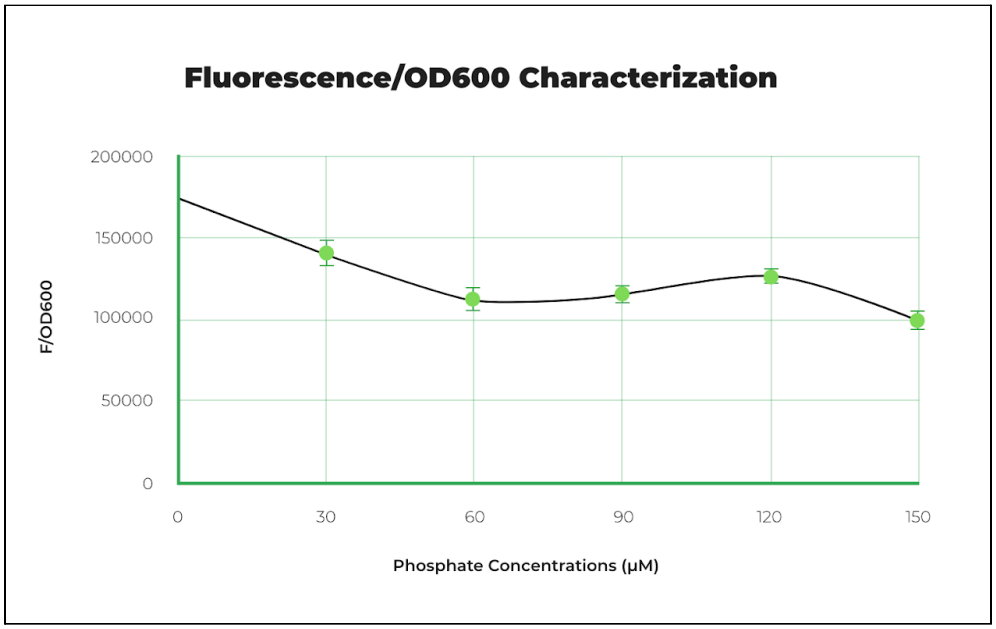

Figure 3.4 *BBa_K2447000 characterization curve showing the relationship between phosphate concentrations between 0µM to150µM and fluorescence/OD$_{600}$.*

Learn

Potential Problems	Solutions
Leaky expression	We proposed to utilize the SsrA degradation tags and the ClpXP ATPase protein mechanisms to break down the GFP reporter protein and prevent leaky expression. The ClpX protein unfolds and translocates the tagged protein into a sequestered proteolytic compartment in ClpP; the ClpP protein breaks the polypeptide bonds that exist between the individual amino acids.
Promoter's low sensitivity to extracellular phosphate	In the event that the BBa_K116401 was not sensitive enough for accurate detection of extracellular phosphate, we researched possible modifications to the promoter. One possibility was to switch the PhoB promoter with a similarly operating PhoA promoter *(See: BBa_K3725110 Design)*. We also proposed to utilize a PhoB consensus sequence to increase the sensitivity of the promoter *(See: BBa_K3725120 Design)*.
Contaminated or incorrectly diluted phosphate solutions	Since our team used the same source of phosphate throughout multiple rounds of characterization, we theorized that the abnormal data was a result of contaminated or incorrectly diluted phosphate solutions. To solve this issue, we remade our phosphate solutions, taking extra caution to prevent contamination and error.
Lack of necessary steps within characterization protocol	While discussing inconsistencies within our protocol, we considered adding MOPS wash steps and a vortex step. The wash steps would reduce the traces of LB surrounding the cell pellets while the vortex step would evenly distribute the cells in our well plate. These steps would increase the overall accuracy within our characterization. *(See: Modified Protocol)*.
Characterization range that is exceeding the biological range of the biosensor	After talking with Dr. Ichiro Matsumura from Emory University and Dr. Mark Styczinski from the Georgia Institute of Technology, concluded that the characterization range of 0μM to 150μM exceeds the natural biological range of the biosensor. They directed us to shift our focus onto a more detailed and accurate characterization for a phosphate concentration range that applies to hydroponics systems. Essentially, we decided that the abnormality around 120μM was out of our control.

Figure 4.1 *Chart showing potential problems of the phosphate biosensor and experimental design and each of their possible solutions.*

Design

BBa_K3725110 Design

Seeking to improve BBa_K2447000, we created BBa_K3725110, an extracellular phosphate sensor with a PhoA promoter and a GFP reporter. The inducible promoter BBa_K1682012, created by 2015 HKUST-Rice iGEM, was originally made to control the expression of the PhoA alkaline phosphatase gene after activation by the phosphorylated PhoB transcription factor. By replacing the downstream PhoA gene with GFP, part BBa_K3725110 also expresses fluorescence in the presence of low levels of extracellular phosphate.

The PhoA construct consists of four basic parts (Figure 5.1): a PhoB-activated promoter (BBa_K1682012), strong RBS (BBa_B0034), GFP reporter (BBa_E0040), and double terminator (BBa_B0015).

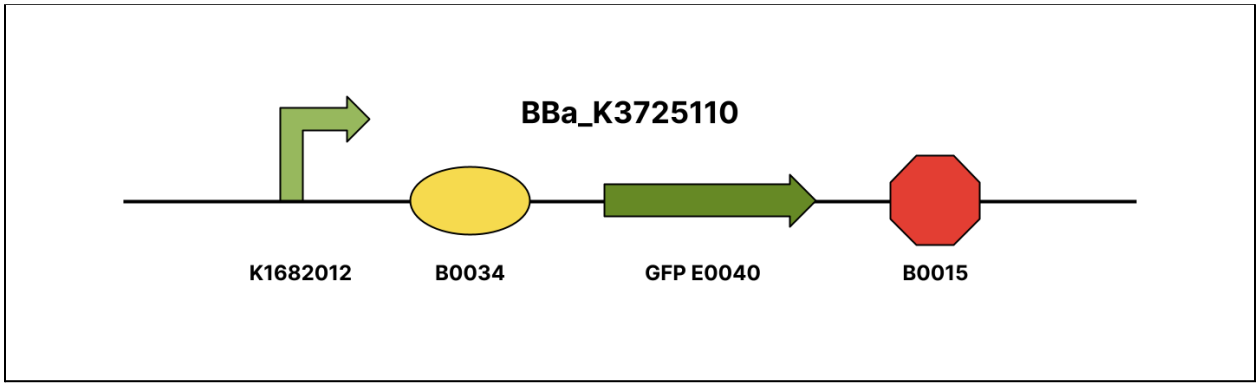

Figure 5.1 *Diagram of the BBa_K3725110 construct.*

BBa_K3725120 Design

We also designed a new phosphate sensor, BBa_K3725120, with a mutated promoter that utilizes a PhoB consensus sequence (Figure 5.2). A consensus sequence is a calculated order of the most repeated nucleotides found at each position in an alignment of multiple other sequences that have a similar function. We engineered the promoter BBa_K3725130 by replacing parts of the PhoB promoter sequence with the PhoB recognition/binding consensus sequence found in literature [3].

Figure 5.2 *Comparison of BBa_K116401 sequence and BBa_K3725130 consensus sequence.*

The BBa_K3725120 construct consists of four basic parts (Figure 5.3): a PhoB-activated consensus promoter (BBa_K3725130), strong RBS (BBa_B0034), GFP reporter (BBa_E0040), and double terminator (BBa_B0015).

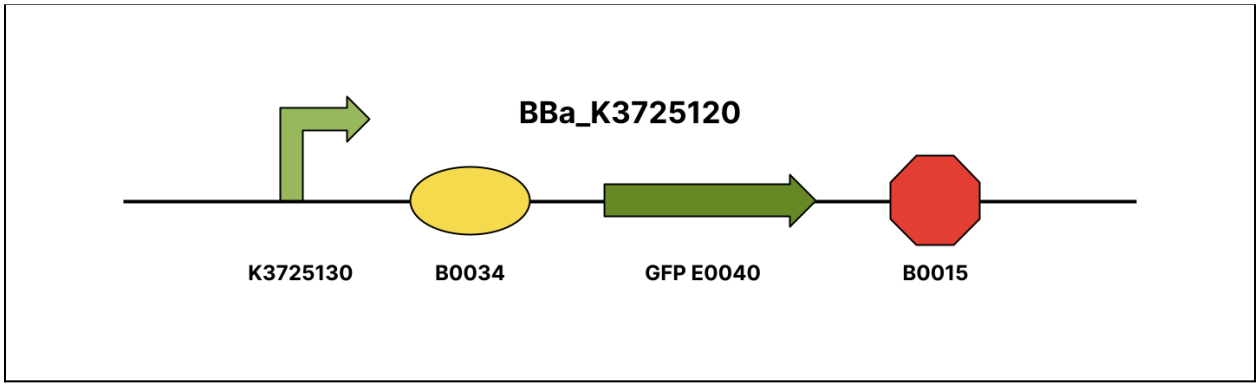

Figure 5.3 *Diagram of the BBa_K3725120 construct.*

Modified Protocol

After extensive discussions with professionals and peers, we concluded that our characterization protocol lacked steps that could reduce errors within our data. As a result, we made two changes to the protocol (Figure 5.4): MOPS wash steps and a vortex step.

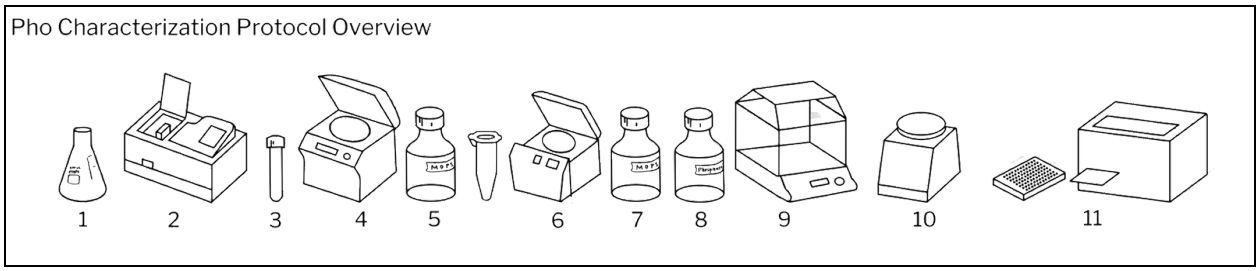

Figure 5.4 *Overview of modified experimental testing protocol.*

The first addition made to the protocol was a series of MOPS wash steps. Originally, we centrifuged the cells, resuspended them in MOPS, and then added phosphate solutions. However, we realized that the MOPS resuspension step did not completely rid traces of the LB media, potentially creating errors in our data since LB contains relatively more phosphate than MOPS. Henceforth, we included MOPS wash steps before adding the phosphate solutions in order to ensure that all or most traces of LB were removed.

The second addition to the protocol was a vortex step before measuring the OD_{600} and fluorescence values of the cells with a plate reader. Since we utilized technical triplicates for our data, an uneven concentration of the cell solution would have resulted in irregular quantification. For this reason, we added a vortex step to ensure that cells were evenly distributed within a well plate before quantification.

Build

BBa_K3725110 Cloning Process

After ordering our part on Integrated DNA Technologies (IDT), we hydrated and transformed the complete plasmid into DH5-alpha competent *E. coli* cells. We then purified and sequenced different colonies from the transformation, and the sequencing results confirmed successful cloning of the part (Figure 6.1).

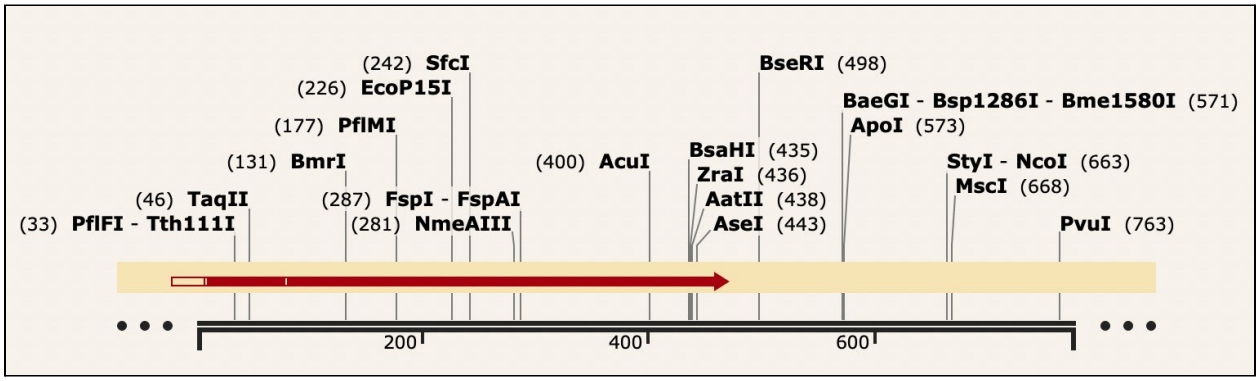

Figure 6.1 *Sequencing results confirming the successful cloning of the BBa_K3725110 part.*

BBa_K3725120 Cloning Process

After ordering our part on Integrated DNA Technologies (IDT), we hydrated and transformed the complete plasmid into DH5-alpha competent *E. coli* cells. Although we attempted to purify and sequence different colonies from the transformation, we noticed that the VF2 primer was not efficient for the sequencing reads. Upon creating a primer specific to our part, we received sequencing results that confirmed successful cloning (Figure 6.2).

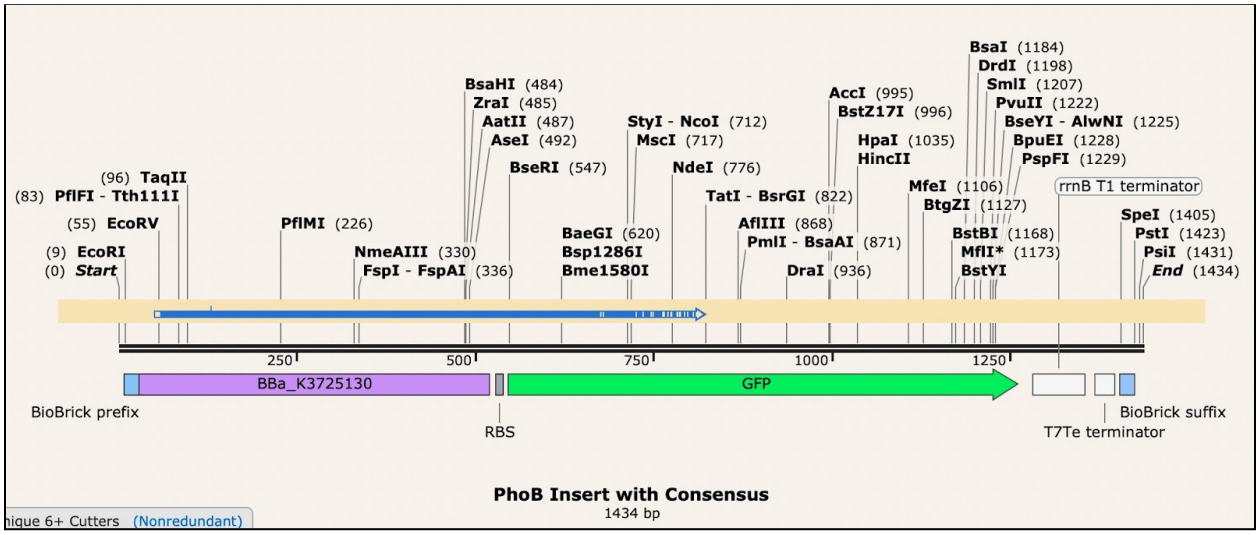

Figure 6.2 *Sequencing results confirming the successful cloning of the BBa_K3725120.*

Test

Comparison Trials

In order to determine the efficiency of the new constructs, we ran comparison trials between the BBa_K2447000 construct and the modified constructs. The trials took place at the same time and within the same conditions to ensure the accuracy of the results.

BBa_K3725110 Characterization

We ran our first comparison trial for BBa_K3725110, utilizing the Modified Protocol. Characterization data from both BBa_K3725110 (Figure 7.1) and BBa_K2447000 (Figure 7.2) revealed negative trends; however, BBa_K3725110 yielded significantly less fluorescence than BBa_K2447000. From this data, we concluded that the PhoA promoter (BBa_K1682012) is less sensitive to extracellular phosphate than the original promoter (BBa_K2447000), thus showing no significant improvement.

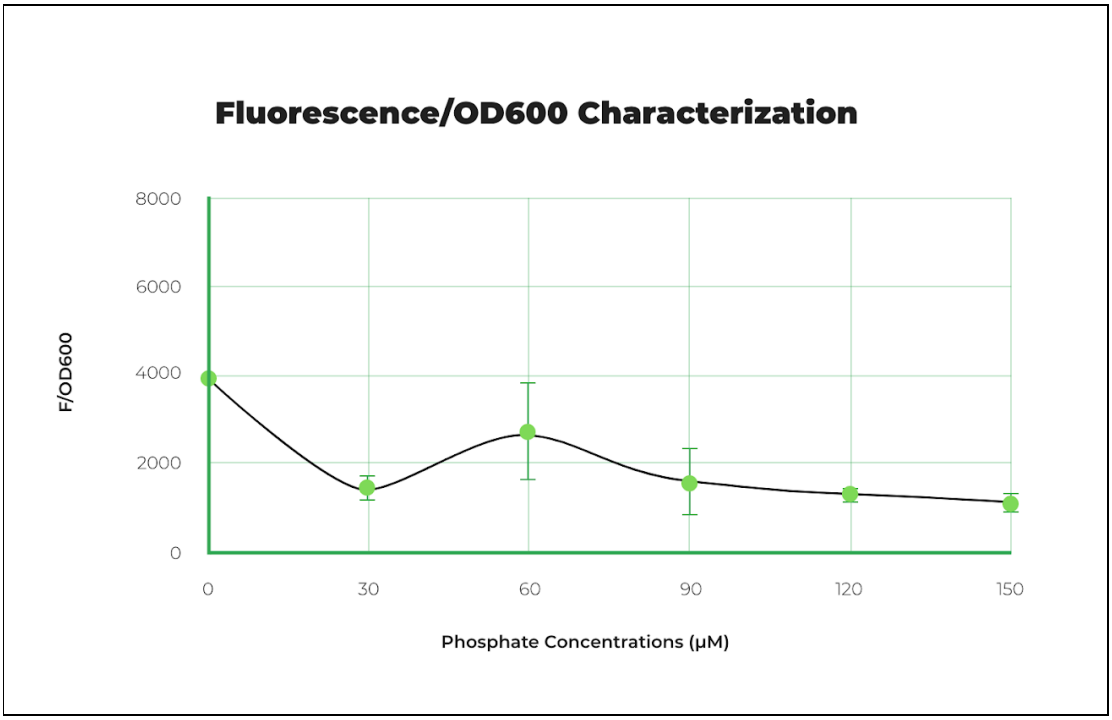

***Figure** 7.1 BBa_K3725110 characterization curve from comparison trials.*

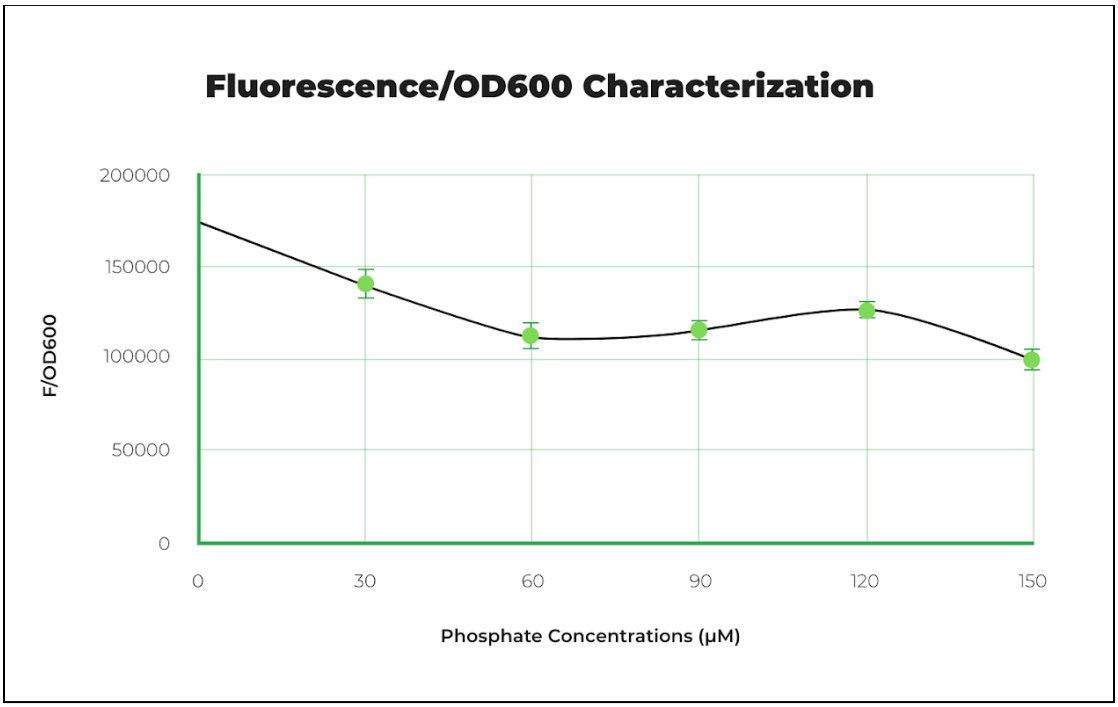

***Figure** 7.2 BBa_K2447000 characterization curve from comparison trials.*

BBa_K3725120 Characterization

For the characterization of BBa_K3725120, we followed the Modified Protocol again. However, after overnight incubation, we noticed that the cells produced no fluorescence. Despite resuspending the cells in MOPS media, which contains relatively less phosphate than LB, the part did not exhibit greater fluorescence. Since we confirmed the cloning of the part with successful sequencing results, we concluded that the part was not efficient as a phosphate sensor and discontinued characterization.

BBa_K2447000 Characterization with Modified Protocol

Using the new protocols mentioned in Modified Protocol, we attempted characterization of BBa_K2447000 again. Comparing the characterization data from the original protocol (Figure 3.5) and that from the modified protocol (Figure 7.3), we noticed an improved curve. The addition of MOPS wash steps and a vortex step allowed us to achieve a more linear characterization curve without abnormalities, while also producing a significantly greater amount of fluorescence.

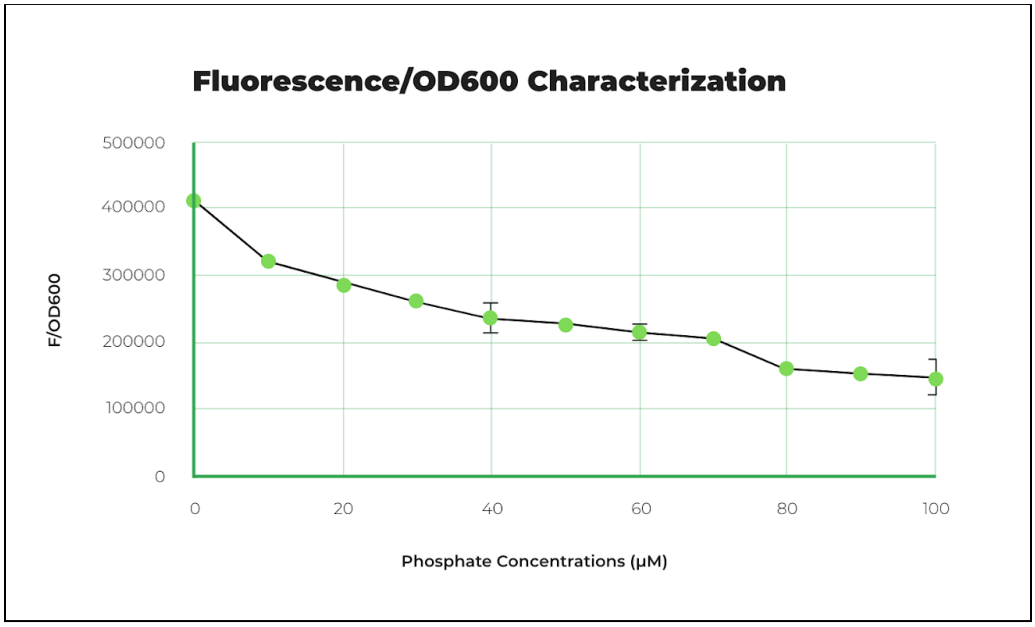

Figure 7.3 *BBa_K2447000 characterization curve using modified protocol.*

Sample Testing

To implement our biosensors into the real world, we experimented with our cells using local water sources, including samples from Dick Creek and Chattahoochee Pointe Park in Forsyth County, Georgia, as well as hydroponics samples from the Sweetwater aeroponics system.

Our phosphate sensor BBa_K2447000 and its characterization curve indicated that the water samples had the following phosphate concentrations:

1. Dick Creek: between 0-10µM
2. Chattahoochee Pointe Park Lake: between 0-10µM
3. Sweetwater Aeroponics System: between 60-70µM

To compare our data to that of a commercial kit, we also utilized the Lamotte phosphate testing kit (Figure 7.4) and identified each samples' phosphate concentrations. The results were as follows:

1. Dick Creek: 1µM
2. Chattahoochee Pointe Park Lake: 0µM
3. Sweetwater Aeroponics System: approximately 50µM

The similar results between analysis with our phosphate sensor and a commercial test kit further substantiated that our biosensor can accurately detect extracellular inorganic phosphate levels, validating its usefulness in regulating hydroponics systems.

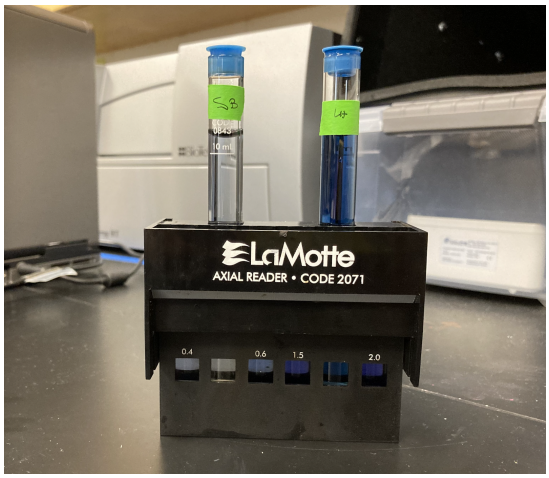

Figure 7.4 *Phosphate concentration analysis for Dick Creek (left) and Lambert Hydroponics (right) using the Lamotte testing kit.*

Lyophilization

BBa_K2447000 also heavily utilizes membrane-bound proteins found within the Pho Regulon signaling pathway. This dependence prevents the sensor from being developed into a cell-free system, making lyophilization a potential solution for safe distribution to the public.

Using LyphoX, we freeze-dried our phosphate biosensor in order to determine whether our cells still function properly after lyophilization. The biosensor properly expressed GFP both before and after lyophilization (Figure 7.5), demonstrating that LyphoX did not compromise the cell structure of the samples. Additionally, successful sequencing results (Figure 7.6) confirmed that the freeze-drying process did not contaminate or denature the DNA (*See: Proof of Concept*).

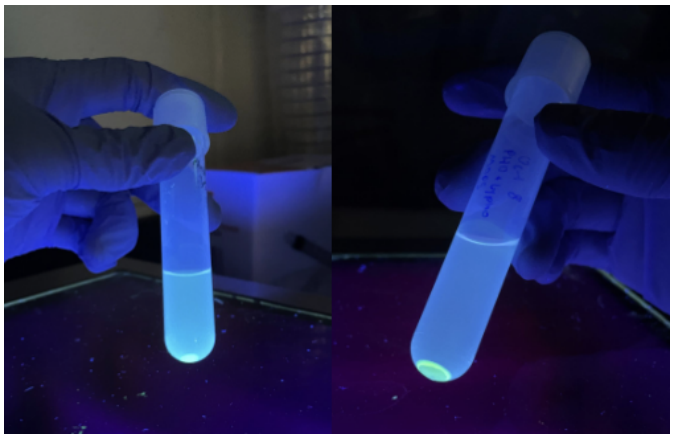

Figure 7.5 *Visible GFP expression of our phosphate sensor before (left) and after (right) lyophilization.*

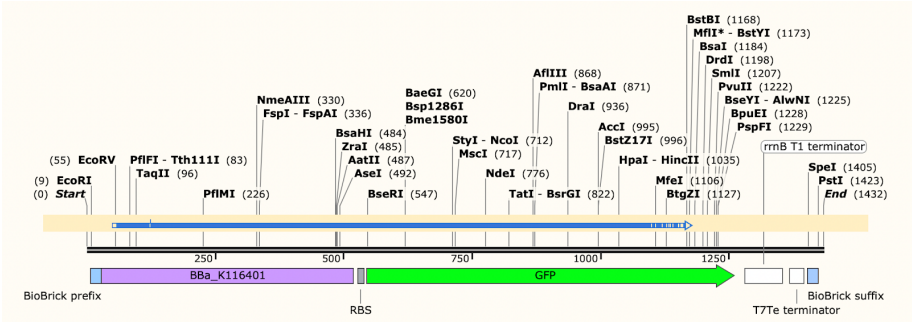

Figure 7.6 *Sequencing results of our phosphate sensor aligned with the original sequence.*

Learn

Potential Problems	Solutions
Incompatible plate reader gain for fluorescence quantification	Through extensive research, we learned that the gain value in a plate reader controls how responsive the device is to the intensity of the quantified sample. Different gains produce similar data trends but change the sensitivity of the data. By quantifying the fluorescence on a range of gains from 25 to 100, we found our characterization data to be optimal at a gain of 100. To promote consistency throughout characterization, we measured fluorescence on a gain of 100 to produce enhanced characterization curves.
Variation of light on different wells of a well plate	In order to confirm there was no variation of light by the plate reader on different wells, we ran a plate variance test. We filled the entire well plate with cells of confirmed, equal cell density and fluorescence. The OD_{600} and fluorescence data revealed no significant outliers, confirming that there were no plate reader trends regarding light variation.
Inefficiency in binding site of the consensus sequence	In the event that the binding site of the consensus sequence was not efficient enough for the PhoB transcription factor, we researched an more efficient consensus sequence. We hypothesized that the mutation in the sequence would cause significant change in the biosensor's activity with the possibility of improving the characterization data.

Figure 8.1 *Chart showing potential problems of the phosphate biosensor and experimental design and each of their possible solutions.*

Design

In an attempt to increase the sensitivity of BBa_3725130 to extracellular phosphate, we designed part BBa_K3725150, a phosphate-sensitive biosensor with modified promoter BBa_K3725140 and GFP reporter. The new promoter utilizes a potentially more efficient consensus sequence (Figure 9.1) by directly mutating the RNS polymerase binding site [4]. The mutation affects the construct's ability to transcribe downstream GFP, thus increasing the sensitivity of the construct and potentially creating an enhanced characterization curve.

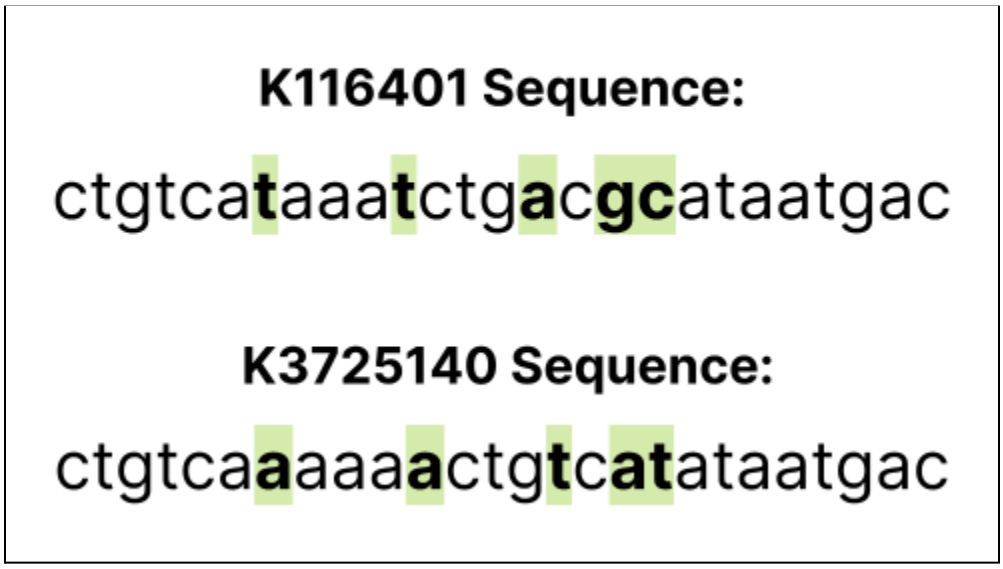

Figure 9.1 *Comparison of BBa_K116401 sequence and BBa_K372140 sequence.*

The new construct consists of four basic parts (Figure 9.2): a redesigned PhoB consensus promoter (BBa_K3725140), strong RBS (BBa_B0034), GFP reporter (BBa_E0040), and double terminator (BBa_B0015).

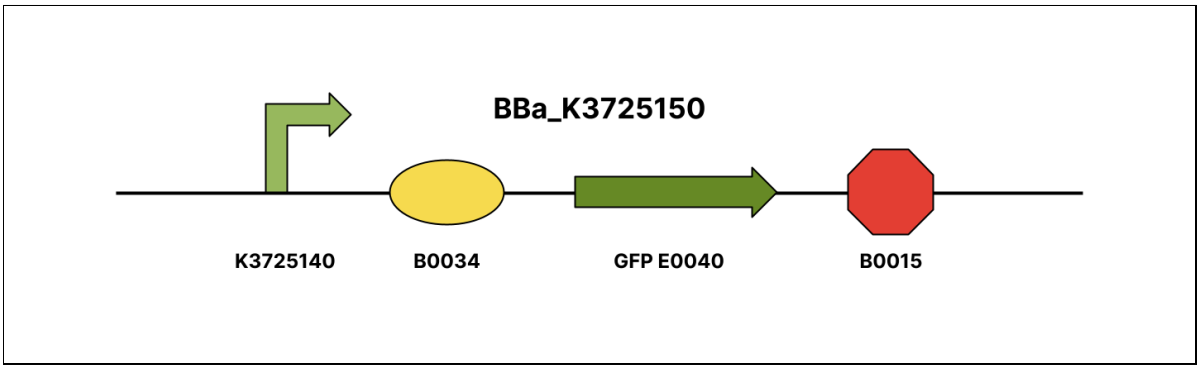

Figure 9.2 *Diagram of the BBa_K3725150 construct.*

Future

In order to continue the development of part BBa_K3725150, we further plan on cloning and characterizing the new biosensor. Our team will run comparison trials between BBa_K3725150 and BBa_K2447000 to further explore the efficacy of the new construct relative to that of our original part.

Ultimately, we hope our biosensor will serve as an cost-effective and accurate method of detection for extracellular phosphate. Our project aims to improve the sustainability and accessibility of hydroponics systems for the exponentially growing population. We hope that our lyophilized biosensor cells will help establish optimal conditions for plant growth in hydroponics and other phosphate-sensitive environments, thus promoting good health and wellbeing of people struggling with food insecurity.

References

[1] Santos-Beneit, F. (2015). The Pho regulon: a huge regulatory network in bacteria. Frontiers in Microbiology, 6. https://doi:10.3389/fmicb.2015.00402.

[2] Uluşeker, C., Torres-Bacete, J., García, J. L., Hanczyc, M. M., Nogales, J., & Kahramanoğulları, O. (2019). Quantifying dynamic mechanisms of auto-regulation in Escherichia coli with synthetic promoter in response to varying external phosphate levels. Scientific Reports, 9(1). https://doi:10.1038/s41598-018-38223-w.

[3] Huang, T.-W., Wen, S.-Y., Chang, C.-Y., Tsai, S.-F., Wu, W.-F., & Chang, C.-H. (2012, October 5). Genome-Wide PhoB Binding and Gene Expression Profiles Reveal the Hierarchical Gene Regulatory Network of Phosphate Starvation in Escherichia coli. PLOS ONE. https://journals.plos.org/plosone/article?id=10.1371%2Fjournal.pone.0047314.

[4] Yuan, Z.-C., Zaheer, R., Morton, R., & Finan, T. M. (2006, May 22). *Genome prediction of PhoB regulated promoters in Sinorhizobium Meliloti and twelve proteobacteria*. Nucleic acids research. Retrieved October 19, 2021, from https://www.ncbi.nlm.nih.gov/pmc/articles/PMC1464414/.